

Microvascular formation in interspaces with different sizes of β -tricalcium phosphate granules used to fill bone defects

Hidehito Yasumitsu, Isumi Toda and Fumihiko Suwa

Department of Anatomy, Osaka Dental University, 8-1 Kuzuhahanazono-cho, Hirakata-shi, Osaka 573-1121, Japan

We investigated how granule interspaces affected vascular formation when a bone defect is filled with different sizes of β -TCP granules. Bone defects in the experimental animals were filled with four sizes of β -TCP granules. Bone and microvascular corrosion cast specimens were then prepared for SEM, and the volume of the newly-formed vascular network was calculated from the SEM images. Newly-formed vasculature was observed in the granule interspaces with all sizes of granules. In particular, the newly-formed vasculature in smaller granules was uniformly distributed. The volume of the newly-formed vasculature was approximately equal in both the experimental and control animals. When β -TCP granules were used to fill bone defects, newly-formed vessels were more uniformly distributed in defects filled with small granules, which are considered advantageous for microvascular formation. (*J Osaka Dent Univ* 2015 ; 49 : 157–164)

Key words : Microvasculature ; Granule interspaces ; β -Tricalcium phosphate ; Bone defect

INTRODUCTION

Bone augmentation is often accomplished by using artificial materials in combination with oral implant treatment.^{1–4} Moreover, placement of implants in the maxilla may require the use of artificial materials for elevation of the maxillary sinus.^{5–8} Beta-tricalcium phosphate (β -TCP) has a high level of osteo-conductivity and is absorbed relatively quickly, to be replaced with autologous bone.^{9–14} It is often used as an artificial material for bone augmentation in dentistry.^{15–21} For bone healing in the extraction socket and growth of tissue around implants, the initial development of microvascular formation is followed by formation of new bone.^{22,23} Microvascular formation advances into the interspaces between the β -TCP granules used to fill the bone defects, resulting in the formation of new bone around the granules.^{24,25} Accordingly, the granule interspaces are considered important for microvascular and new bone formation. We speculated that microvascular formation in the granular interspaces might vary depending on the size of the granules used. In the present study, we used β -

TCP granules of different sizes to fill bone defects in experimental animals, and investigated the relationship between granule interspace size and microvascular formation.

MATERIALS AND METHODS

Materials

Four sizes of β -TCP granules were used ; Types P (50–150 μm), S (200–500 μm), M (500–1,000 μm) and L (1,000–2,000 μm) (Fig. 1). The Type P granules (Kyocera Medical, Kyoto, Japan) were the compact type, while the Type S, M and L granules (BIORESORB[®] Macro Pore ; ORALTRONICS, Bremen, Germany) each had a porosity of 30%, as they consisted of micropores of 0.5–10 μm (mean 5 μm) and macropores of 50–700 μm (mean 500 μm), both of which are referred to as ‘macropores’ for convenience in the present study.

Experimental animals

Five adult male crab-eating monkeys with an average body weight of 5 kg and healthy permanent dentition in both the upper and lower jaws were used. The bilat-

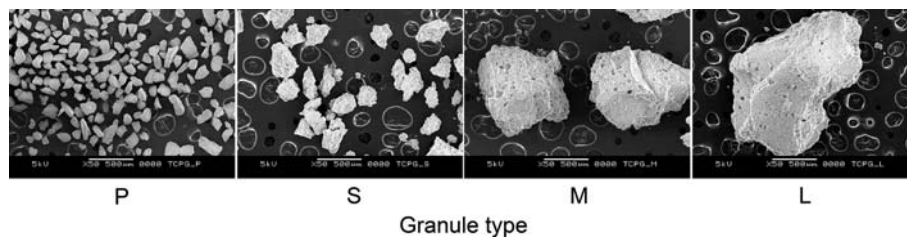


Fig. 1 SEM images of β -TCP granule types P, S, M and L (Bars = 500 μ m).

eral lower molars were used as experimental sites. The animals were given a standard primate diet (PS-A, Oriental Yeast, Tokyo, Japan) and water. The present experiment was approved by the Animal Research Committee of Osaka Dental University (Approval numbers 13-02001 and 14-02001) and performed under the provisions of the Regulations for Animal Experiments of Osaka Dental University.

Methods

Surgical procedures

The five monkeys were given general anesthesia using 0.1 mL/kg injection of 2% xylazine hydrochloride (Selactal[®]; Bayer Yakuin, Tokyo, Japan) as a sedative and 0.2 mL/kg ketamine hydrochloride (Ketalar[®]; Daiichi Sankyo Propharma, Tokyo, Japan) as an anesthetic. The bilateral lower molars (second premolar, first molar and second molar) were extracted to minimize surgical invasion of the surrounding tissue. For 1 week after surgery, mouth rinsing was performed daily with a 0.01% benzethonium chloride solution (Neostelin Green Gargle 0.2%[®]; Nippon Shika Yakuin, Shimonoseki, Japan) and the animals were given a soft diet. As an antimicrobial agent for preventing infection, injection of 15 mg/kg lincomycin hydrochloride hydrate (Lincocin[®]; Pfizer Japan, Tokyo, Japan) was administered intramuscularly.

At eight weeks after tooth extraction, the animals were again anesthetized using the same procedure as that for tooth extraction. The gingiva in the experimental region was incised and detached to expose the bone, and a total of 6 bone defects, 3 on each side, were formed by drilling to a depth of 6 mm in the buccal socket margin using a 3.5-mm implant drill (ITI implant system; STRAUMANN, Basel, Switzerland) under irrigation with physiological saline (Otsuka nor-

mal saline injection; Otsuka Pharmaceutical, Tokushima, Japan). Granules in physiological saline were used to fill the defects, with Type L and S granules separately placed in the two defects on one side, and Type P and M granules on the other side. The remaining two defects on each side were left unfilled to serve as controls. After filling with the granules, a gingival flap was sutured over the wound to complete the procedure. Similar to the situation after tooth extraction, intraoral rinsing was performed and a soft diet was given for the first week after surgery, while an antibacterial agent was administered intramuscularly to prevent infection. The suture was removed at 1 week after surgery and the soft diet was replaced with a standard primate diet. The animals were then housed for 1 more week (Fig. 2).

Preparation of samples

At two weeks after the second procedure, the five monkeys were euthanized by injection of an overdose of 50 mg/kg pentobarbital sodium salt (Somnopen[®]; Kyoritsu Seiyaku, Tokyo, Japan), and then acrylic resin was injected through the bilateral carotid artery using a microvascular injection method.^{26,27} After the resin hardened, the animals were soaked in 10% neutral buffer formalin solution and the experimental regions were extracted using a large diamond band saw (BS-310 CP; EXAKT, Norderstedt, Germany). Blocks of each bone defect, both filled and unfilled, were prepared using a small diamond band saw (BS-3000; EXAKT).

Granule interspace measurement

Among the cut blocks, those filled with granules were radiographed using a micro focus X-ray CT system (micro-CT) (SMX-130 CT; SHIMADZU, Kyoto, Ja-

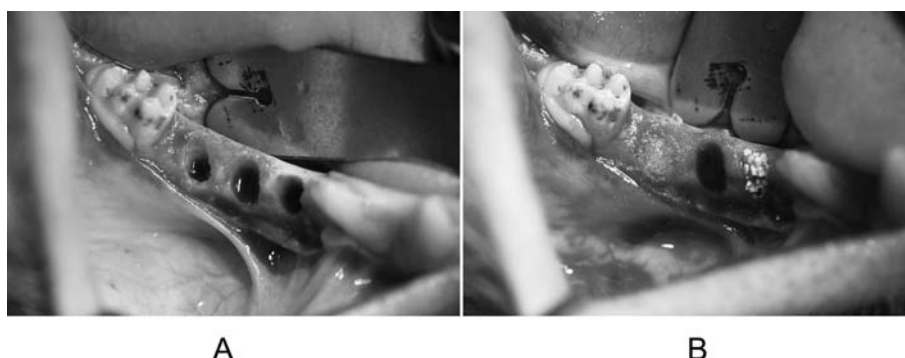


Fig. 2 Bone defects in an experimental animal (right side). (A) Immediately after creation of defects (three defects), (B) Defects filled with granules (Type M, Control, and Type P from medial to distal).

pan) with a tube voltage of 45 kV, a tube current of 120 μ A, and a slice thickness of 27.5 μ m. Slice images of only the bone defect portions were separated and processed into 3D images using 3D image analysis software (VGStudio MAX[®] Ver.1.2.1 ; Volume Graphics, Heidelberg, Germany). Furthermore, to highlight only the granule interspaces in the images, a columnar portion 3 mm in diameter and 5 mm in height was extracted by removing the surrounding area contacting the socket wall of the defect. The volume of the granules and that of the interspaces in the columnar portion was then determined. The dimension of the interspaces was calculated from the mean for the X, Y and Z axes.

Preparation of specimens for scanning electron microscopy

The bone defect portion of each block obtained from one of the experimental animals was cut at the center to obtain frontal sections. One was left untreated and the other was decalcified with 5% hydrochloric acid. For specimens from the remaining four animals, each block was cut horizontally into four slices of thickness 1.5 mm, and the bottom and middle slices were selected as samples (Fig. 3). The sample slices were soaked in 5% sodium hypochlorite to dissolve and remove soft tissue, then rinsed with water and dried. These were used as bone and microvascular cast specimens. After evaporating with osmium tetroxide using a plasma multi coater (PMC-5000 ; Meiwa, Osaka, Japan), the specimens were observed under a scanning electron microscope (SEM) (JSM-5500 ;

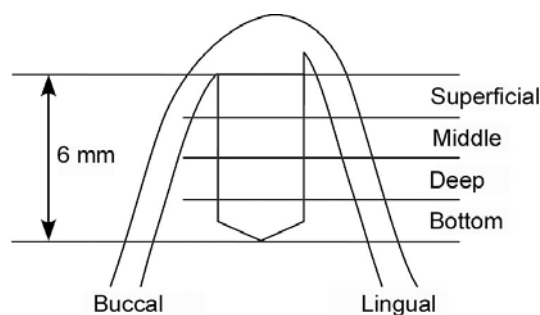


Fig. 3 Schematic illustration of the bone defect regions. The bone defect was separated horizontally into four regions (superficial, middle, deep and bottom) to make the specimens.

JEOL, Tokyo, Japan) at an accelerating voltage of 5 kV and working distance of 48 mm. Digital images were obtained for observation from a cross-section of frontal sections and from the top surface of horizontal sections. Furthermore, horizontal section specimens were soaked in 5% hydrochloric acid to remove hard tissue. After rinsing in water and drying, they were used as microvascular cast specimens. Following gold coating (JFC-1500 ; JEOL, Tokyo, Japan), they were observed with an SEM and digital images were obtained.

Image analysis of newly-formed vessels in granule interspaces

Based on SEM images of the microvascular casts as decalcified horizontal-section specimens, the bone defect portion was extracted using photo retouch software (Photoshop[®] ; Adobe Systems, San Jose, CA, USA) on a personal computer (MacBook Pro, Apple

Computer, Cupertino, CA, USA). The ratio of the area of newly-formed vessels to the area of bone defect was calculated using binary images of the vessels and public domain image analysis software (Image J; National Institutes of Health, Bethesda, MD, USA). The mean dimensions for the interspace between each type of granule were calculated and used as the amount of newly-formed vessels.

RESULTS

Granule interspace measurements (Table 1)

The mean dimensions of the interspace between granules used to fill the bone defects in the experimental animals were 96.4 ± 4.3 , 151.2 ± 5.6 , and $243.2 \pm 15.4 \mu\text{m}$ for Types S, M and L, respectively. It was impossible to measure the interspace between the Type P granules using the 3D image analysis software employed in the present study.

SEM images (Figs. 4, 5 and 6)

Type P granules

Although SEM images of the non-decalcified specimens showed newly-formed vessels in the granule interspaces, granules were missing in some areas at the time of specimen preparation. SEM images of the decalcified specimens showed newly-formed vessels oriented toward the center of the bone defect in a uniform manner (Figs. 4 and 5).

Type S granules

SEM images of the non-decalcified specimens showed newly-formed vessels in the granule interspaces, some of which had invaded the macropores in the granules. SEM images of the decalcified specimens showed newly-formed vessels oriented toward the center of the bone defects in a uniform manner (Figs. 4, 5 and 6).

Table 1 Granule interspace dimensions

Granule type	Average	X-axis	Y-axis	Z-axis
S	96.4 ± 4.3	98.2 ± 3.4	99.8 ± 7.7	92.0 ± 4.5
M	151.2 ± 5.6	153.0 ± 8.1	152.8 ± 6.1	148.4 ± 11.1
L	243.2 ± 15.4	240.0 ± 16.0	240.0 ± 16.2	251.0 ± 20.8

Mean \pm SD, n = 5 (μm)

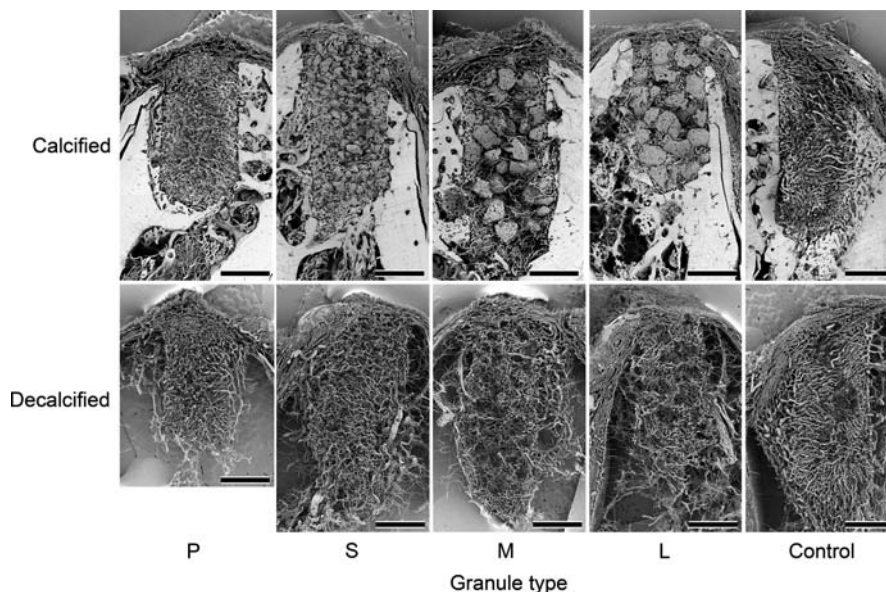


Fig. 4 SEM images of sagittal sections (Bar = 2 mm).

Type M granules

SEM images of the non-decalcified specimens showed newly-formed vessels in the granule interspaces, some of which had invaded the macropores in the granules. SEM images of the decalcified specimens showed that areas of newly-formed vessels were absent, which corresponded to the granules. New vessels formed in the interspaces appeared to encircle the granules (Figs. 4, 5 and 6).

Type L granules

SEM images of the non-decalcified specimens showed newly-formed vessels in the granule interspaces in the same manner as observed for the Type M granules. Some of the vessels had invaded the macropores in the granules. SEM images of the decalcified specimens showed that areas of newly-formed vessels were absent, which corresponded to the granules, the same as seen with Type M gran-

ules. New vessels formed in the interspaces appeared to encircle the granules (Figs. 4, 5 and 6).

Controls

SEM images of the non-decalcified specimens showed formation of new vessels oriented nearly uniformly toward the center of the bone defect. Similarly, SEM images of the decalcified specimens showed newly-formed vessels that appeared to be nearly the same as those seen in the non-decalcified specimens (Figs. 4 and 5).

Vascular invasion of macropores

SEM images of the non-decalcified specimens for the Type S, M and L granules, in which macropores were present, showed newly-formed vessels invading the macropores (Fig. 6). Measurements of the invaded macropores using image analysis software (Image Pro[®] Plus, Ver. 5.1 ; Media Cybernetics, Rockville,

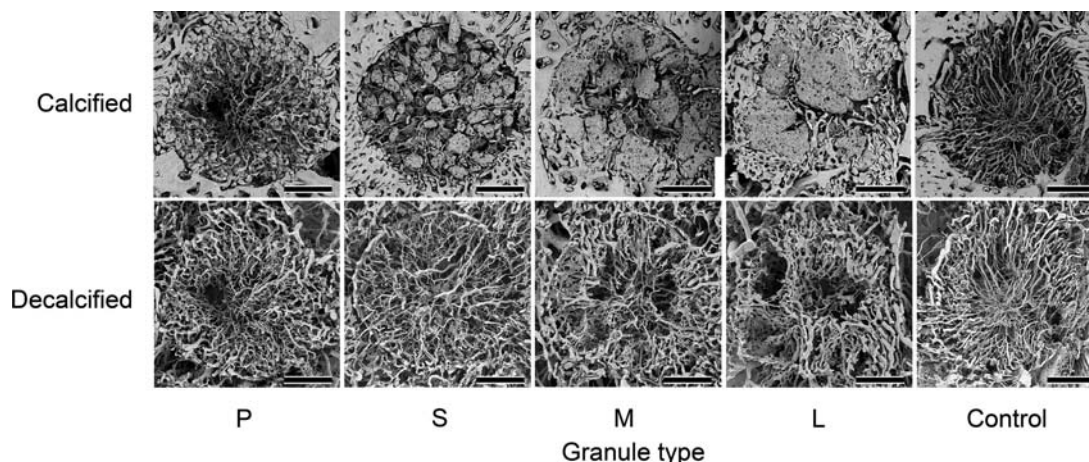


Fig. 5 SEM images of horizontal sections (Bar = 1 mm).

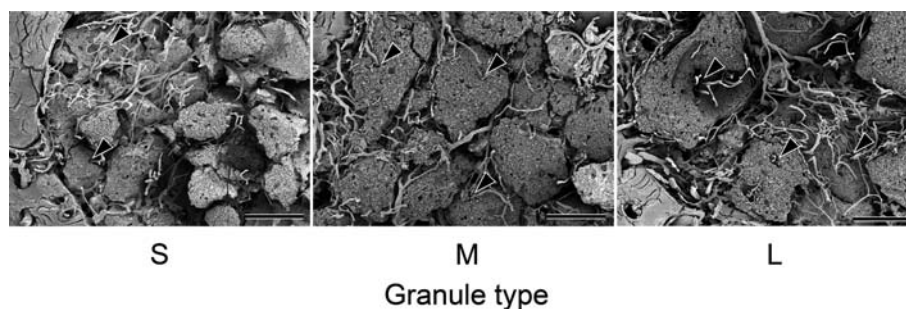


Fig. 6 Close-up SEM images of horizontal sections of calcified specimens showing the granules filling the defect. Newly formed vessels (arrow heads) invaded the macropores in the granules (Bar = 500 μ m).

Table 2 Diameter of macropores invaded by newly formed vessels

Granule type	S	M	L
Diameter	38.9 ± 12.7	42.1 ± 12.1	39.6 ± 13.9

Mean ± SD, n = 8 (μm)

Table 3 Ratio of newly formed vessels in the bone defect

Granule type	P	S	M	L	Control
Area (%)	20.0 ± 5.0	20.0 ± 4.5	17.5 ± 4.6	17.9 ± 6.7	20.0 ± 2.9

Mean ± SD, n = 8

MD, USA) showed them to be 38.9 ± 12.7 , 42.1 ± 12.1 , and $39.6 \pm 13.9 \mu\text{m}$ in diameter for the Type S, M and L granules, respectively. One-way ANOVA revealed no significant differences among the three sizes of granules (Table 2). In contrast, no macropores or vascular invasion was observed in specimens with the Type P granules.

Ratio of newly-formed vessels as determined by image analysis (Table 3)

The ratio of newly-formed vessels in the granule interspaces calculated on the basis of SEM images of horizontally sectioned decalcified specimens was $20.0 \pm 5.0\%$, $20.0 \pm 4.5\%$, $17.5 \pm 4.6\%$, $17.9 \pm 6.7\%$, and $20.0 \pm 2.9\%$ for Type P, S, M and L granules and the controls, respectively. One-way ANOVA revealed no significant difference among the specimens for different granule sizes.

DISCUSSION

Animal experiment

The period from 1 to 2 weeks after surgery is considered to be the stage of microvascular formation during bone healing around the extraction socket and implant, while the stage of new bone formation and bone remodeling begins at about 2 weeks, after which bone healing is completed.^{22, 23} Accordingly, based on findings of animal experiments of bone defects filled with β -TCP granules, we think that microvascular formation in the granule interspaces could be confirmed by preparing samples obtained at 2 weeks after surgery, which would be the stage of microvascular for-

mation just prior to new bone formation. Furthermore, we think that newly-formed vessels in the bone defects could be clearly determined by use of specimens prepared following acrylic resin microvascular injection.^{26, 27}

Granule interspace measurements

Granule interspace measurements based on micro-CT findings performed at 2 weeks showed that the interspaces in defects filled with Type S, M and L granules became larger in accordance with granular size. We also found that the mean interspace measurement for Type S granules was greater than $90 \mu\text{m}$, while it was previously reported that granules larger than $50 \mu\text{m}$ are required for microvascular formation in the pores.²⁸ Thus, we concluded that microvascular formation could be sufficiently attained with use of the Type S, M and L granules employed in the present study.

On the other hand, determination of interspaces with the Type P granules was impossible, even though imaging was performed under the same conditions as for the other types. The cause for this failure seems to be related to the compact nature of the Type P granules, as radiolucency was low with the high granule density in the bone defects. As a result, interspaces smaller than $27 \mu\text{m}$ were unrecognizable, since the slice thickness of the specimens subjected to micro-CT was $27.5 \mu\text{m}$. Granule interspaces smaller than $27 \mu\text{m}$ could not be clearly visualized.

Relationship between granule interspaces and microvascular formation

SEM images of the non-decalcified specimens confirmed newly-formed vessels in the granule interspaces of all defects filled with Type P, S, M and L granules. Even with Type P granules, for which interspace measurements based on 3D image analysis was impossible, newly-formed vessels were observed in the interspaces. Accordingly, we speculate that even a granule interspace size of $27 \mu\text{m}$ or less may be adequate for microvascular formation.

SEM images of the decalcified specimens showed areas free from newly-formed vessels corresponding to the granules in those with Type M and L granules,

in which newly-formed vessels in the interspaces were observed encircling the granules. Meanwhile with Type S and P granules there were no newly-formed vessels encircling the granules, as the vessels were spread throughout the bone defects. This was thought to be the result of microvascular formation in the finely distributed interspaces of the defects filled with Type S and P granules, which were relatively small in size.

Relationship between granular interspaces and the amount of microvascular formation

There was no significant difference in the amount of newly-formed vessels among the granule types. The ratio was about 20% for Types P and S, which was the same as that of the controls, while the ratios were a bit smaller for Types M and L, at 17% and 18%, respectively. These findings suggest that the size of the interspaces is not always proportional to the amount of newly-formed vessels.

In the controls, new vessels were formed nearly uniformly in the bone defects, as there was no factor to inhibit microvascular formation. As shown in the SEM images of decalcified specimens, microvascular formation occurred nearly uniformly in specimens with Types P and S. It seems that the amount of newly-formed vessels with this size of granules is approximate, as microvascular formation was uniform in the uniformly distributed interspaces formed by small-sized granules, as was also seen in the controls. Meanwhile, in specimens with Types M and L, it seems that the amount of newly-formed vessels was less, because microvascular formation occurred in the disproportionately larger interspaces formed by the larger granules.

Vascular invasion of macropores in granules

The Type S, M and L granules used in the present study had a porosity of 30%, and contained intragranular macropores of two size ranges, 0.5–10 μm and 50–700 μm . SEM images of the non-decalcified specimens confirmed vascular invasion of intragranular macropores. The average size of macropores that showed invasion was 40 μm , with no significant differences among the types. It has been re-

ported that macropores larger than 50 μm are required for microvascular formation.²⁸ However, in the present specimens, vessel invasion was noted in macropores 40 μm in diameter. Even at 2 weeks after surgery, when granular resorption had already been initiated and the macropores in the granules were as small as 0.5–10 μm , the macropores were thought to grow larger to make invasion by new vessels possible.

When using β -TCP granules to fill bone defects, larger granules with higher porosity and larger macropores are considered better for microvascular formation than small granules like Type P and S. This is because the newly-formed vessels are more uniformly distributed in defects filled with the larger Type M and L granules, making a greater amount of newly-formed vessels. We intend to perform another study in the future on the relationship between microvascular formation and new bone formation during the new bone formation stage using the present methods to determine the optimum conditions for β -TCP granule filling of bone defects, such as granule size, porosity, and interspace size.

We are grateful to the members of the Department of Anatomy for their kind advice and assistance.

REFERENCES

1. Hempton TJ, Fugazzotto PA. Ridge augmentation utilizing guided tissue regeneration, titanium screws, freeze-dried bone, and tricalcium phosphate : clinical report. *Implant Dent* 1994 ; **3** : 35–37.
2. Hardwick R, Hayes BK, Flynn C. Devices for dentoalveolar regeneration : an up-to-date literature review. *J Periodontol* 1995 ; **66** : 495–505.
3. Mercier P, Bellavance F, Cholewa J, Djokovic S. Long-term stability of atrophic ridges reconstructed with hydroxylapatite : a prospective study. *J Oral Maxillofac Surg* 1996 ; **54** : 960–968.
4. Scarano A, Carinci F, Assenza B, Piattelli M, Murmura G, Piattelli A. Vertical ridge augmentation of atrophic posterior mandible using an inlay technique with a xenograft without miniscrews and miniplates : case series. *Clin Oral Implants Res* 2011 ; **22** : 1125–1130.
5. Yildirim M, Spiekermann H, Biesterfeld S, Edelhoff D. Maxillary sinus augmentation using xenogenic bone substitute material Bio-Oss[®] in combination with venous blood. A histologic and histomorphometric study in humans. *Clin Oral Implants Res* 2000 ; **11** : 217–229.
6. Tadjoedin ES, de Lange GL, Holzmann PJ, Kuiper L, Burger EH. Histological observations on biopsies harvested following sinus floor elevation using a bioactive glass material of narrow

- size range. *Clin Oral Implants Res* 2000 ; **11** : 334–344.
7. Hallman M, Cederlund A, Lindskog S, Lundgren S, Sennerby L. A clinical and histologic study of bovine hydroxyapatite in combination with autogenous bone and fibrin glue for maxillary sinus floor augmentation. Results after 6 to 8 months of healing. *Clin Oral Implants Res* 2001 ; **12** : 135–143.
 8. Szabó G, Suba Z, Hrabák K, Barabás J, Németh Z. Autogenous bone versus β -tricalcium phosphate graft alone for bilateral sinus elevations (2- and 3-dimensional computed tomographic, histologic, and histomorphometric evaluations): Preliminary results. *Int J Oral Maxillofac Implants* 2001 ; **16** : 681–692.
 9. Nagahara K. Osteogenesis in response to tricalcium phosphate (TCP) and hydroxyapatite ceramics (HAP) implanted into bone tissues. *Shika Kiso Igakkai Zasshi (Jpn J Oral Biol)* 1987 ; **29** : 131–155. (Japanese)
 10. Oyake Y, Beppu M, Ishii S, Takagi M, Takashi M. Intramedullary anchoring strength of titanium rod with mixed β -tricalcium phosphate and fibrin adhesive. *J Orthop Sci* 2002 ; **7** : 123–130.
 11. Ozawa M. Experimental study on bone conductivity and absorbability of the pure β -TCP. *Seitai Zairyo (J Jpn Soc Biomaterial)* 1995 ; **13** : 167–175. (Japanese)
 12. Saito M, Shimizu H, Beppu M, Takagi M. The role of β -tricalcium phosphate in vascularized periosteum. *J Orthop Sci* 2000 ; **5** : 275–282.
 13. Dong J, Uemura T, Shirasaki Y, Tateishi T. Promotion of bone formation using highly pure porous β -TCP combined with bone marrow-derived osteoprogenitor cells. *Biomaterials* 2002 ; **23** : 4493–4502.
 14. Morikawa S. Comparative study on β -tricalcium phosphate and hydroxyapatite as bioactive artificial bone fillers. *Tokyo Jikei-kai Ika Daigaku Zasshi (Tokyo Jikeikai Med J)* 2000 ; **115** : 193–207. (Japanese)
 15. Ormianer Z, Palti A, Shifman A. Survival of immediately loaded dental implants in deficient alveolar bone sites augmented with β -tricalcium phosphate. *Implant Dent* 2006 ; **15** : 395–403.
 16. Brkovic BMB, Prasad HS, Konandreas G, Milan R, Antunovic D, Sándor GKB, Rohrer MD. Simple preservation of a maxillary extraction socket using beta-tricalcium phosphate with type I collagen : preliminary clinical and histomorphometric observations. *J Can Dent Assoc* 2008 ; **74** : 523–528.
 17. Horowitz RA, Mazor Z, Miller RJ, Krauser J, Prasad HS, Rohrer MD. Clinical evaluation of alveolar ridge preservation with a β -tricalcium phosphate socket graft. *Compend Contin Educ Dent* 2009 ; **30** : 588–603.
 18. Honda K. Clinical study of a novel bone augmentation with β -tricalcium phosphate. *Okayama Shigakkai Zasshi (J Okayama Dent Soc)* 2009 ; **28** : 1–9. (Japanese)
 19. Frenken JWFH, Bouwman WF, Bravenboer N, Zijdeveld SA, Schulten EAJM, ten Bruggenkate CM. The use of Straumann® Bone Ceramic in a maxillary sinus floor elevation procedure : a clinical, radiological, histological and histomorphometric evaluation with a 6-month healing period. *Clin Oral Implants Res* 2010 ; **21** : 201–208.
 20. Wakimoto M, Ueno T, Hirata A, Iida S, Aghaloo T, Moy PK. Histologic evaluation of human alveolar sockets treated with an artificial bone substitute material. *J Craniofac Surg* 2011 ; **22** : 490–493.
 21. Hirota M, Matsui Y, Mizuki N, Kishi T, Watanuki K, Ozawa T, Fukui T, Shoji S, Adachi M, Monden Y, Iwai T, Tohnai I. Combination with allogenic bone reduces early absorption of β -tricalcium phosphate (β -TCP) and enhances the role as a bone regeneration scaffold. Experimental animal study in rat mandibular bone defects. *Dent Mater J* 2009 ; **28** : 153–161.
 22. Suwa F. Bone healing around dental implant –microvascularization and bone formation in functional or non functional conditions–. *Nihon Shika Igakkai Shi (J Jpn Assoc Dent Sci)* 1998 ; **17** : 124–129. (Japanese)
 23. Suwa F. What is discovered from microvascular corrosion cast-bone specimens. *Denshi Kenbikyo (Electron Microscopy)* 1999 ; **34** : 168–172. (Japanese)
 24. Kuroki K, Toda I, Suwa F. Experimental study of bone defect repair process with different sizes of β -TCP granules. *Nihon Koku Implant Gakkai Shi (J Jpn Soc Oral Implant)* 2008 ; **21** : 21–31. (Japanese)
 25. Toda I, Yasuda K, Ehara D, Kuroki K, Suwa F. The effects on extraction sockets filled with small β -tricalcium phosphate granules : An experimental histomorphometric study. *Nihon Koku Implant Gakkai Shi (J Jpn Soc Oral Implant)* 2013 ; **26** : 228–235. (Japanese)
 26. Ohta Y, Okuda H, Suwa F, Okada S, Toda I. Plastic injection method for preparing microvascular corrosion casts for SEM and its practical application. *Okajimas Folia Anat Jpn* 1990 ; **66** : 301–312.
 27. Suwa F, Uemura M, Takemura A, Toda I, Fang YR, Xu YJ, Zhang ZY. Acrylic resin injection method for blood vessel investigation. *Okajimas Folia Anat Jpn* 2013 ; **90** : 23–29.
 28. Ehara Y, Suwa F. Experimental studies on the osseous restoration and microvascular formation after dental implantation of the pored alumina ceramics. *Shika Kiso Igakkai Zasshi (Jpn J Oral Biol)* 1994 ; **36** : 471–485. (Japanese)